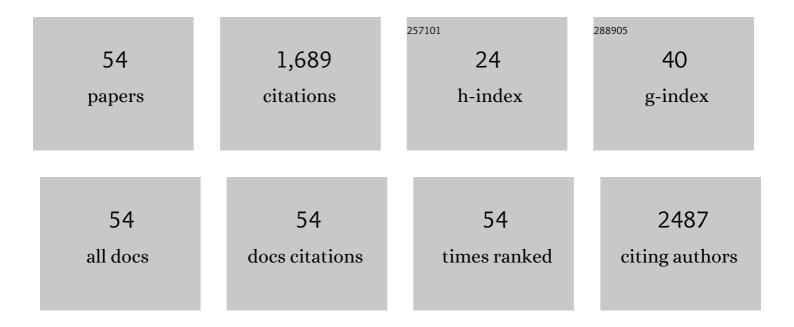
MiguelÃ;ngel Gracia-Pinilla

List of Publications by Year in descending order

Source: https://exaly.com/author-pdf/4653557/publications.pdf Version: 2024-02-01



#	Article	IF	CITATIONS
1	Solar photocatalytic activity of TiO2 modified with WO3 on the degradation of an organophosphorus pesticide. Journal of Hazardous Materials, 2013, 263, 36-44.	6.5	163
2	Effective removal of phosphate from aqueous solution using humic acid coated magnetite nanoparticles. Water Research, 2017, 123, 353-360.	5.3	127
3	Synthesis by sol–gel of WO3/TiO2 for solar photocatalytic degradation of malathion pesticide. Catalysis Today, 2013, 209, 35-40.	2.2	115
4	Mechanothermal synthesis of Ag/TiO2 for photocatalytic methyl orange degradation and hydrogen production. Chemical Engineering Research and Design, 2018, 120, 339-347.	2.7	106
5	Deposition of Size-Selected Cu Nanoparticles by Inert Gas Condensation. Nanoscale Research Letters, 2010, 5, 180-188.	3.1	99
6	Highly size-controlled synthesis of Au/Pd nanoparticles by inert-gas condensation. Faraday Discussions, 2008, 138, 353-362.	1.6	98
7	Influence of mesoporous defect induced mixed-valent NiO (Ni2+/Ni3+)-TiO2 nanocomposite for non-enzymatic glucose biosensors. Sensors and Actuators B: Chemical, 2018, 264, 27-37.	4.0	88
8	Kinetic and Mechanistic Evaluation of Inorganic Arsenic Species Adsorption onto Humic Acid Grafted Magnetite Nanoparticles. Journal of Physical Chemistry C, 2018, 122, 13540-13547.	1.5	54
9	On the Structure and Properties of Silver Nanoparticles. Journal of Physical Chemistry C, 2008, 112, 13492-13498.	1.5	48
10	Sonophotocatalytic (42kHz) degradation of Simazine in the presence of Au–TiO2 nanocatalysts. Applied Catalysis B: Environmental, 2014, 160-161, 692-700.	10.8	47
11	Construction of direct Z-scheme WO3/ZnS heterojunction to enhance the photocatalytic degradation of tetracycline antibiotic. Journal of Environmental Chemical Engineering, 2021, 9, 105111.	3.3	47
12	UV and Visible Light-Driven Production of Hydroxyl Radicals by Reduced Forms of N, F, and P Codoped Titanium Dioxide. Molecules, 2019, 24, 2147.	1.7	46
13	Synthesis, characterization, photocatalytic evaluation, and toxicity studies of TiO2–Fe3+ nanocatalyst. Journal of Materials Science, 2014, 49, 5309-5323.	1.7	42
14	Low frequency ultrasound (42 kHz) assisted degradation of Acid Blue 113 in the presence of visible light driven rare earth nanoclusters loaded TiO2 nanophotocatalysts. Ultrasonics Sonochemistry, 2014, 21, 1675-1681.	3.8	39
15	Sonochemical synthesis of CuO nanostructures and their morphology dependent optical and visible light driven photocatalytic properties. Journal of Materials Science: Materials in Electronics, 2017, 28, 2448-2457.	1.1	36
16	Hydrogen adsorption properties of Ag decorated TiO2 nanomaterials. International Journal of Hydrogen Energy, 2018, 43, 2861-2868.	3.8	35
17	Heterostructures of mesoporous TiO2 and SnO2 nanocatalyst for improved electrochemical oxidation ability of vitamin B6 in pharmaceutical tablets. Journal of Colloid and Interface Science, 2019, 542, 45-53.	5.0	35
18	Deactivation of Ni-SiO2 catalysts that are synthetized via a modified direct synthesis method during the dry reforming of methane. Applied Catalysis A: General, 2020, 594, 117455.	2.2	35

#	Article	IF	CITATIONS
19	Preparation of nanosized yttrium doped CeO2 catalyst used for photocatalytic application. Journal of Saudi Chemical Society, 2015, 19, 505-510.	2.4	34
20	Industrial synthesis and characterization of nanophotocatalysts materials: titania. Nanotechnology Reviews, 2016, 5, 467-479.	2.6	31
21	Size-Selected Ag Nanoparticles with Five-Fold Symmetry. Nanoscale Research Letters, 2009, 4, 896-902.	3.1	29
22	Sonophotocatalytic mineralization of Norflurazon in aqueous environment. Chemosphere, 2016, 146, 216-225.	4.2	28
23	Enhanced photo-induced catalytic activity of Cu ion doped ZnO - Graphene ternary nanocomposite for degrading organic dyes. Journal of Water Process Engineering, 2019, 32, 100966.	2.6	27
24	Sonophotocatalytic degradation of Acid Blue 113 in the presence of rare earth nanoclusters loaded TiO2 nanophotocatalysts. Separation and Purification Technology, 2014, 133, 407-414.	3.9	26
25	Photosynthesis of H2 and its storage on the Bandgap Engineered Mesoporous (Ni2+/Ni3+)O @ TiO2 heterostructure. Journal of Power Sources, 2020, 466, 228305.	4.0	23
26	Fluorine-free synthesis of reduced graphene oxide modified anatase TiO2 nanoflowers photoanode with highly exposed {0 0 1} facets for high performance dye-sensitized solar cell. Solar Energy, 2020, 211, 1017-1026.	2.9	18
27	Ultrasound assisted synthesis of morphology tunable rGO:ZnO hybrid nanostructures and their optical and UV-A light driven photocatalysis. Journal of Luminescence, 2017, 186, 53-61.	1.5	17
28	Heterogeneous sonocatalytic activation of peroxomonosulphate in the presence of CoFe2O4/TiO2 nanocatalysts for the degradation of Acid Blue 113 in an aqueous environment. Journal of Environmental Chemical Engineering, 2020, 8, 104024.	3.3	15
29	Synthesis, characterization, and photocatalytic performance of FeTiO3/ZnO on ciprofloxacin degradation. Journal of Photochemistry and Photobiology A: Chemistry, 2021, 411, 113186.	2.0	14
30	CuO-ZnO-PANI a lethal p-n-p combination in degradation of 4-chlorophenol under visible light. Journal of Hazardous Materials, 2021, 416, 125989.	6.5	14
31	Realization of structural transformation for the enhancement of magnetic and magneto capacitance effect in BiFeO3–CoFe2O4 ceramics for energy storage application. Scientific Reports, 2021, 11, 2265.	1.6	12
32	Synthesis, characterization, and visible light–induced photocatalytic evaluation of WO3/NaNbO3 composites for the degradation of 2,4-D herbicide. Materials Today Chemistry, 2021, 19, 100406.	1.7	12
33	Effect of rare earth dopants on structural and mechanical properties of nanoceria synthesized by combustion method. Materials Science & Engineering A: Structural Materials: Properties, Microstructure and Processing, 2016, 649, 168-173.	2.6	11
34	Magnetically recyclable CoFe ₂ O ₄ /ZnO nanocatalysts for the efficient catalytic degradation of Acid Blue 113 under ambient conditions. RSC Advances, 2020, 10, 16473-16480.	1.7	10
35	Low frequency ultrasound assisted sequential and co-precipitation syntheses of nanoporous RE (Gd) Tj ETQq1 1	0.784314 1.7	rgBT /Overlo
36	Influence of RE (Pr3+, Er3+, Nd3+) doping on structural, vibrational and enhanced persistent photocatalytic properties of ZnO nanostructures. Spectrochimica Acta - Part A: Molecular and Biomolecular Spectroscopy, 2022, 268, 120679.	2.0	9

#	Article	IF	CITATIONS
37	Effective degradation of cefuroxime by heterogeneous photo-Fenton under simulated solar radiation using α-Fe2O3-TiO2. Journal of Environmental Chemical Engineering, 2021, 9, 106822.	3.3	9
38	Microstructure, vibrational and visible emission properties of low frequency ultrasound (42 kHz) assisted ZnO nanostructures. RSC Advances, 2016, 6, 20437-20446.	1.7	8
39	Effect of Sr 2+ and Ba 2+ doping on structural stability and mechanical properties of La 2 NiO 4+Î′. Ceramics International, 2018, 44, 10551-10557.	2.3	7
40	Graphene induced band gap widening and luminescence quenching in ceria:graphene nanocomposites. Journal of Alloys and Compounds, 2019, 770, 1221-1228.	2.8	7
41	Probing the Defect-Induced Magnetocaloric Effect on Ferrite/Graphene Functional Nanocomposites and their Magnetic Hyperthermia. Journal of Physical Chemistry C, 2019, 123, 25844-25855.	1.5	7
42	Spray-assisted layer-by-layer assembly of decorated PEI/PAA films: morphological, growth and mechanical behavior. Journal of Coatings Technology Research, 2017, 14, 927-935.	1.2	6
43	Photocatalysis as an effective advanced oxidation process. Water Intelligence Online, 2017, 16, 333-381.	0.3	6
44	Morphology controlled synthesis of Sm doped ZnO nanostructures for photodegradation studies of Acid Blue 113 under UV-A light. Journal of Materials Science: Materials in Electronics, 2015, 26, 8784-8792.	1.1	5
45	Long-term influence of chitin concentration on the resistance of cement pastes determined by atomic force microscopy. Physica Status Solidi (A) Applications and Materials Science, 2016, 213, 3110-3116.	0.8	5
46	A facile hydrothermal synthesis of CeO2 nanocubes decorated ZnO nanostructures: optical and enhanced photocatalytic properties. Journal of Materials Science: Materials in Electronics, 2019, 30, 11643-11651.	1.1	5
47	Structural, electrical, ferroelastic behavior, and multiferroic properties of BiFeO3. Journal of Materials Science: Materials in Electronics, 2020, 31, 13141-13149.	1.1	5
48	Structural studies on the gadolinium doped nanoceria prepared by combustion synthesis. Materials Letters, 2014, 125, 19-24.	1.3	4
49	Influence of refluxing time and HMTA on structural and optical properties of rod, prism like ZnO nanostructures. Journal of Materials Science: Materials in Electronics, 2019, 30, 5670-5680.	1.1	4
50	Spectroscopic Investigation on rGO:ZnO Composites Nanostructures. Springer Proceedings in Physics, 2017, , 63-69.	0.1	3
51	Structural and mechanical properties of La0.6Sr0.4M0.1Fe0.9O3-δ (M: Co, Ni and Cu) perovskites. Ceramics International, 2017, 43, 2089-2094.	2.3	3
52	Synthesis and Characterization of NiCr Self-Assembled Nanorings. Journal of Nano Research, 2010, 9, 101-108.	0.8	2
53	Structural investigation and sonocatalytic efficiency of Ce 0.9 Nd 0.1 O 1.95 and Ce 0.9 Pr 0.1 O 1.95 nanocatalysts. Materials Chemistry and Physics, 2017, 200, 241-249.	2.0	2
54	Water Disinfection Using Chitosan Microbeads With N-, C-, C-N/TiO2 By Photocatalysis Under Visible Light. Topics in Catalysis, 2021, 64, 142-154.	1.3	2